Anal. Bioanal. Electrochem., Vol. 8, No. 6, 2016, 675-690

Analytical & Bioanalytical Electrochemistry

2016 by CEE
www.abechem.com

Full Paper

Fabrication of Titanium Dioxide Nanofiber Composite and Using in Modified Carbon Paste Electrode for Determination of Tryptophan in the Presence of Penicillamine and Folic acid

Mohammad Mazloum-Ardakani* and Rezvan Arazi

Department of Chemistry, Faculty of Science, Yazd University, Yazd, 89195-741, I.R. Iran

*Corresponding Author, Tel.: +983518211670; Fax: +983518210644

E-Mail: mazloum@yazd.ac.ir

Received: 18 June 2016 / Received in revised form: 19 August 2016 / Accepted: 22 August 2016 / Published online: 30 September 2016

Abstract- In this present work, we prepared a carbon paste modified electrode with 9,10-dihydroxy-7-methoxy-6H-benzofuro[3,2-c]chromen-6-one (DMC) and titanium dioxide nanofiber composite (DMC/NF/CP) as a electrochemical sensor for electrochemically sensitive and selective detection of tryptophan (Trp.) in the presence of penicillamine (PA) and folic acid (FA). The modified CPE was successfully used to determine the concentrations of Trp., PA and FA in real samples. The electron transfer rate constant, k_s, and transfer coefficient, α, were calculated to be 1.88 s^{-1} and 0.6 respectively, by cyclic voltammetry measurements. The catalytic peak current obtained from differential pulse voltammetry (DPV was linearly towards the Trp. concentration in the range of 1.0-900.0 μM. The detection limit (3σ) for Trp. was 0.103 μM with a sensitivity of 0.128 μA μM^{-1}.

Keywords- Electrochemical sensor, Nanofiber, Tryptophan, Penicillamine, Folic acid

1. INTRODUCTION

The importance of nanotechnology has gained new and widely fields for the application of nanomaterials in analytical chemistry [1–3]. The similar dimensions of nanomaterials and protein molecules offer that the integration of the two will cause to attractive new materials.

The fascinating physical and chemical properties of nanomaterials suggest excellent prospects for a wide range of bio-sensing applications [4–7].

Nanofibers are attractive for various applications due to their intrinsically high surface area to mass or volume ratio and high porosities. Electrospinning is a low cost, versatile and simple process to generate nanofibers from different materials including polymers, ceramics and composites [8,9]. A rich variety of polymers are used to electrospun with sol-gel chemistry to generate composite and inorganic nanofibers [10]. These composite nanofibers such as poly(vinyl pyrrolidone) (PVP), poly(vinyl acetate) (PVAc), poly(vinyl alcohol) (PVA) or poly(ethylene oxide) (PEO) can be electrospun from sol-gel precursor solutions and calcinated in air to remove organic phase. Various inorganic components such as SiO_2, SnO_2, TiO_2, ZnO, Nb_2O_5 and Al_2O_3 are used to prepare composite nanofibers [11]. During the electrospinning, a polymer solution flows out from needle, which is connected to a syringe and a high voltage causes that the charge to be induced within the polymer and polymer pulled onto a collector by strong electric field and form nanofibers structure. The electrospun nanofibers diameters are depended on a number of various parameters that include:

1- The properties of the solution such as solvent and the type of polymers, polymer molecular weight, concentration (or viscosity), conductivity, elasticity and surface tension [12].
2- The operation conditions such as distance between the tip and the collecting, applied voltage and flow rate [13].
3- The environmental conditions consist of humidity and temperature has an important role in quality of prepared nanofiber.

Tryptophan (2-amino-3-(1H-indol-3-yl)-propionic acid, Trp.) is a vital and essential component of proteins and imperative in human nutrition to establish and maintain a positive nitrogen balance. Abnormal levels of serotonin and melatonin have been shown to be associated with depression and Alzheimer's and Parkinson's diseases, respectively [14]. Therefore, various methods have been applied to the determination of Trp., such as colorimetric [15] and ultraviolet detection [16]. These methods have many advantages of sensitivity and accuracy, but their high cost, complicated operations and time-consuming limit their widely application for routine and benefit Trp. analysis. However, electrochemical method for detection of Trp. has gained attractive due to its low expense, simplicity, high sensitivity, and possibility of miniaturization [17–20] compared to the mentioned methods. It is obvious that the electrochemical determination of Trp. at the unmodified electrode is not arbitrary because of sluggish electron transfer processes and high over-potential [21,22]. To dominate the problems of selectivity and sensitivity, the electrode surface can be modified to decrease the overpotential, enhance the mass transfer velocity and effectively enrich the substance [23–25].

D-Penicillamine (2-amino-3-mercapto-3-methylbutanoic acid, PA), a well-known chelating agent, is belongs to the amino-thiol family. It is a treatment of cystinuria, Wilson's disease by acting as a chelating agent which is used to aid the elimination of copper [26], fibrotic lung diseases, rheumatoid arthritis, primary biliary cirrhosis, scleroderma certain forms of metal intoxication and progressive systemic sclerosis [27]. Different methods have been to detection of PA in both pharmaceutical preparations and biological samples. These methods include spectrophotometry [28], capillary electrophoresis [29], chemiluminescence [30] and electrochemical methods [31,32].

Folic acid or folate ((2S)-2-[(4-{[(2-amino-4-hydroxypteridin-6-yl) methyl] amino}phenyl)formamido] pentanedioic acid, FA) is a B vitamin. Folic acid is essential for numerous bodily functions. Humans cannot synthesize folates, therefore folic acid has to be supplied through the diet to meet their daily requirements. The human body needs folate to synthesize DNA, repair DNA, and methylate DNA as well as to act as a cofactor in certain biological reactions. Low levels of folate can also lead to homocysteine accumulation and associated with specific cancers [33].

In this paper, we reported a nanostructure electrochemical sensor decorated by titania nanofiber composite for simultaneous determination of Tryptophan in the presence of penicillamine and folic acid for the first time. The use of the modified electrode in this report provides a simple and sensitive method for the detection of Trp.. In addition, the kinetics of the mediated electrooxidation of Trp. at this type of mediator–modified carbon paste electrode is investigated using cyclic voltammetry measurements. Our findings indicate that the DMC/NF/CP give several distinct advantages, including an extraordinary high surface charge transfer rate constant and good limit of detection for Trp.. Also, the modified electrode exhibited excellent electrochemical activity towards sensitive detection of Trp. in real samples.

2. EXPERIMENTAL

2.1. Apparatus and chemicals

Electrochemical experiments were carried out using a potentiostat/galvanostat μAutolab type III (Eco Chemie B.V.A) controlled with General Purpose Electrochemical System (GPES) software. A conventional three electrode cell was used including modified electrode, Ag/AgCl/KCl (3.0 M, Azar electrode, Iran), and a Pt wire (Azar electrode, Iran) as working, reference and counter electrodes, respectively. Trp., PA, FA and all other reagents were analytical grade from Merck (Darmstadt, Germany). The graphite powder and paraffin oil, both from Merck (Darmstadt, Germany). The preparation of nanofibers were performed by using an electrospinning setup (FNM Co., Iran), which is controlling the flow rates, voltage and distance between tip and collector (Scheme 1). Scanning electron microscopy (SEM) was

used to characterization of nanomaterials (TESCAN SEM system). X-ray diffraction (XRD) patterns of products were obtained by a Philips diffractometer utilizing X'PertPro and the monochromatized Cu Kα radiation.

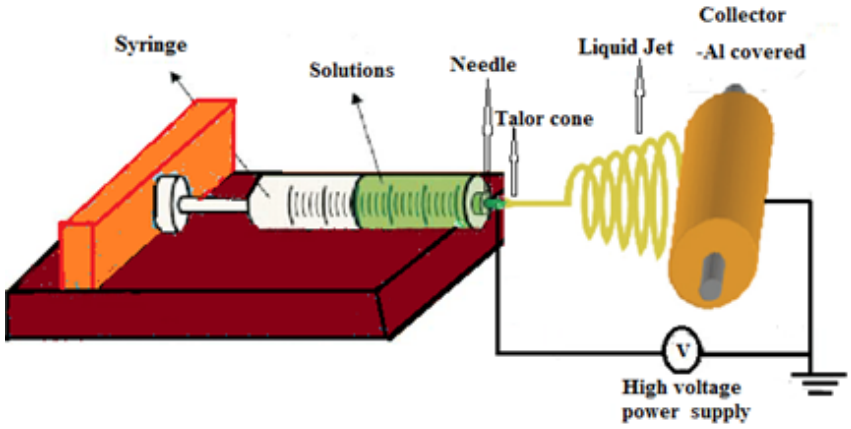

Scheme 1. Schematic of a typical electrospinning setup

2.2. Synthesis of 9,10-dihydroxy-7-methoxy-6H-benzofuro [3,2-c]chromen-6-one (DMC)

DMC was synthesized by electrosynthesis method and the manner described in our previous work [32]. Briefly, 60 mL of 0.15 M phosphate buffer (pH 7.0) in water/acetonitrile (85/15 volume ratio), containing 0.5 mmol of 4-methoxybenzene-1, 2-diol and 0.5 mmol 4-hydroxycoumarin was electrolyzed at controlled-potential (0.35 *vs*. SCE) in a divided cell. The electrolysis was terminated when the current decayed to 5% of its original value. The precipitated solid was collected by filtration and was washed several times with water.

2.3. Preparation of different electrodes

The DMC/NF/CP was prepared by hand mixing 0.005 g of DMC with 0.5 g graphite powder and 0.005 g of nanofiber with a mortar and pestle. Then ~0.7 mL of paraffin was added to this mixture and the mixture was ground for 20 min until a uniform paste was obtained. The paste was then packed into the end of a glass tube. The electrical contact was provided by pushing a copper wire down the glass tube into the back of the carbon paste. For electrical measurement, by pushing an excess of paste out of the tube and polishing it with a weighting paper, a new surface was obtained. For comparison, a NF modified CPE (NF/CP), DMC modified CPE (DMC/CP), DMC/NF modified CPE (DMC/NF/CP) and bare CPE were prepared in the same way but without addition of NF, DMC and both DMC and NF respectively.

2.4. Preparation of nanofiber

Nanofiber was prepared according to the procedures described in the literature [35], briefly Poly(vinyl pyrrolidone) (PVP, Mw=1,300,000, was dissolved in 4 mL ethanol (EtOH, Merck, 99.8%) and 1 mL N, N-dimethylformamide (DMF, Merck, 99.8%). A solution of titanium isopropoxide (TiP, 98%, Aldrich) with the metal contents of 50.69 wt% was prepared by stirring and 2 mL acetic acid was added to the solution to get a transparent solution. Then, this solution was added into PVP solution and stirring for 5 h at room temperature to enhance its viscosity. The distance between the Al foil and the spinneret was 10 cm and the applied voltage was 15 KV. A flow rate of 0.5 mL/h was controlled using a syringe pump. The nanofibers were deposited on the Al foil, dried at 80 °C for 4 h to evaporate their solvents and calcined in 600 °C at the rate of 2 °C /min for 2 h and utilized as a nanocomposite on carbon paste electrode to determine some biological species.

3. RESULTS AND DISCUSSION

3.1. SEM and XRD characterization

Fig. 1 is shown SEM images of different electrodes.

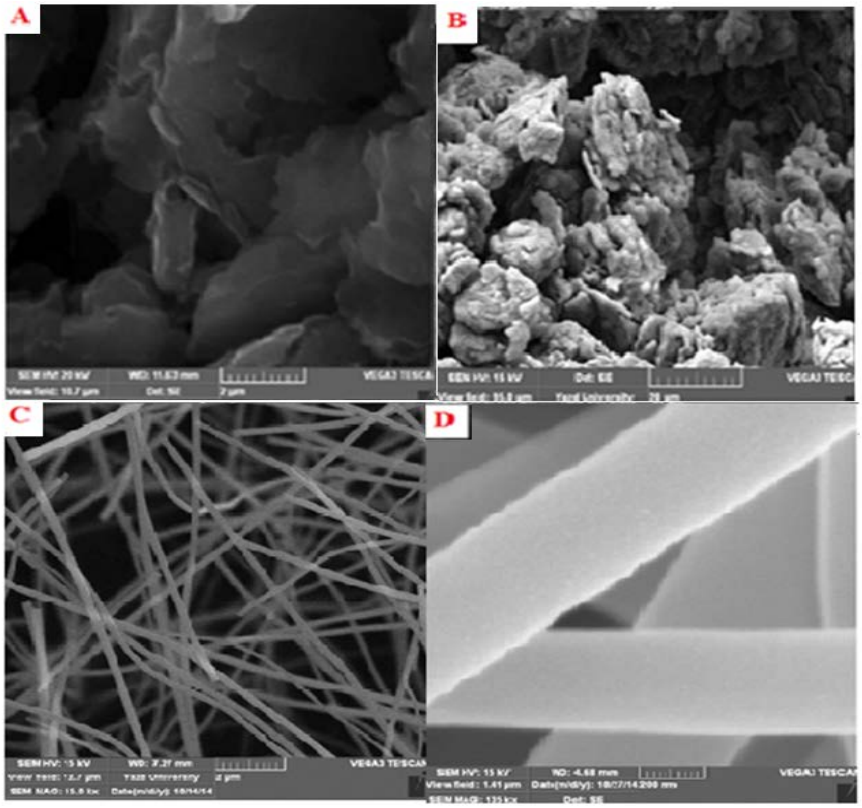

Fig. 1. SEM images of different carbon paste electrodes. CPE (A), CPE-NF (B), calcinated TiO_2 nanofibers (600 °C) (C), TiO_2 nanofiber with large magnification (D)

As shown in Fig. 1A, after nanofiber added to the carbon paste electrode (Fig. 1B) the distribution of these components on the paste can be seen and the ratio of area to volume has been increased clearly. After optimizing the critical preparation parameters, the TiO_2 nanofibers composite are obtained and the SEM micrographs of calcinated (600 °C) nanofibers are shown in Fig. 1C and 1D. These images show ultrafine and smooth fibers with the great roughness and high surface area. Fig. S1 (in supporting information) is shown the XRD results of TiO_2 nanofibers that were electrospun from an ethanol solution containing 1 mL TiP and PVP (0.45 g), subsequently calcinated for 2 h at 600 °C in air. The nanocrystalline anatase structure was confirmed by (1 0 1), (0 0 4), (2 0 0), (1 0 5) and (2 1 1) diffraction peaks [36]. The XRD patterns of anatase has a main peak at 2θ=25.28 corresponding to the 101 planes (JCPDS 21-1272) while the main peaks of rutile and brookite phases are at 2θ=27.48 (110 plane) and 2θ=30.88 (1 2 1 plane). The prominent peaks representing anatase /rutile phase of nanocrystalline TiO_2 powder used for this study can be seen at the 2θ values of 25.28, 27.48, 37 80, 48.05, 53.89, 55.06, 62.69, 68.76, 70.31 and 75.03.

3.2. Voltammetric behaviors of the DMC/NF/CP

Cyclic voltammograms of the DMC/NF/CP in a 0.1 M phosphate buffer solution (pH 7.0) at various scan rates are shown in Fig. 2. In this Fig., the anodic and cathodic currents increase linearly with scan rates from 10 to 3000 mVs^{-1} (Fig. 2, inset A) as predicted for a diffusionless system, indicating that the modified electrode exhibits electrochemical responses with characteristics of the redox species confined on the electrode surface. The anodic (I_{pa}) and cathodic peak currents (I_{pc}) were linearly dependent on scan rate. Fig. 2, inset B, shows the magnitudes of the peak potentials (E_p) as a function of the logarithm of the potential scan rate. The slopes of inset C plots in Fig. 2, can be used to extract the kinetic parameters α_c (cathodic transfer coefficients) and $\alpha=1-\alpha_c$ (anodic transfer coefficients). The slope of the linear segment is equal to $2.303RT/\alpha nF$ for the anodic and $-2.303RT/\alpha_c F$ for the cathodic peak. The calculated value for the coefficient α is 0.6. The apparent charge transfer rate constant, k_s, for the electron transfer between the modified electrode and the DMC can be determined from CV experiments using the variation of the oxidation and reduction peak potentials with the logarithm of scan rates according to the Laviron theory [37]. Equation (1) can be used to determine the electron transfer rate constant, k_s:

$$\log k_s=\alpha\log(1-\alpha)+(1-\alpha)\log\alpha-\log(RT/nF\upsilon)-\alpha(1-\alpha)n_\alpha F\Delta E_p/2.3RT \quad (1)$$

Where $(1-\alpha)n_\alpha=0.4$, ν is the sweep rate, and all other symbols have their conventional meanings. k_s was calculated to be 1.88 s^{-1}.

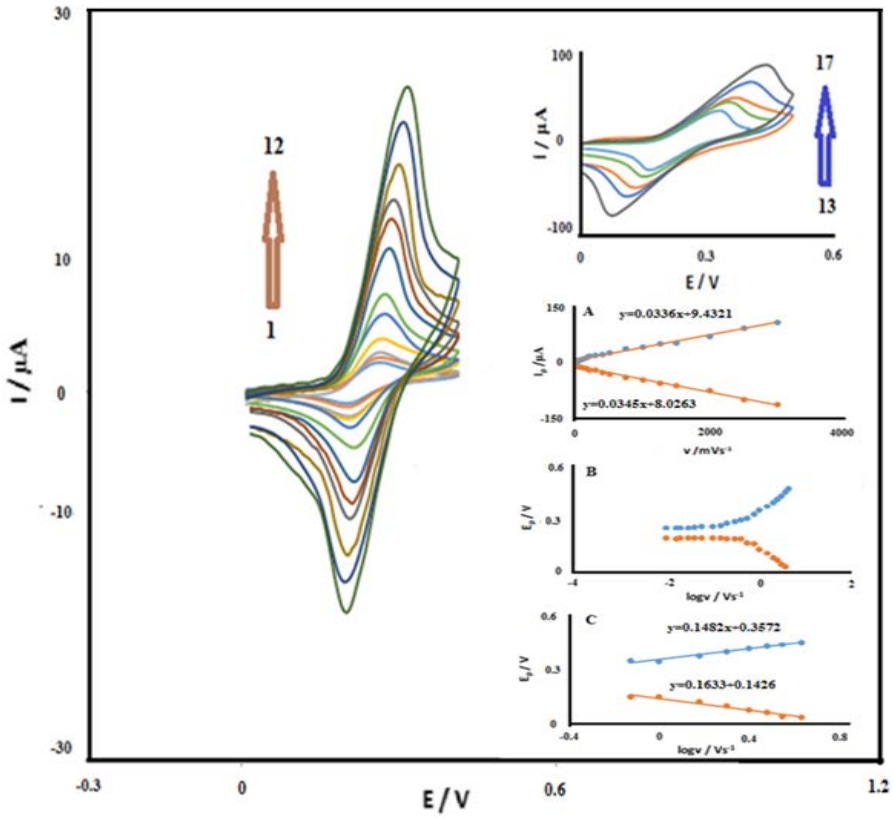

Fig. 2. Cyclic voltammograms of DMC/NF/CP in 0.1 M phosphate buffer (pH 7.0) at scan rates: (1) 10, (2) 20, (3) 30, (4) 40, (5) 50, (6) 100, (7) 150, (8) 200, (9) 300, (10) 400, (11) 500, (12) 750, (13) 1000, (14) 1250, (15) 1500, (16) 2000, and (17) 2500 mVs^{-1}. Insets: (A) Variation of peak currents with sweep rate. (B) Variation of E_p *vs*. the logarithm of the scan rate. (C) Magnification of the same plot for high scan rates

3.3. Influence of pH

The effect of pH value of the supporting electrolyte solution on the DMC/NF/CP signal was also investigated by cyclic voltammetry using a 0.l M phosphate buffer with increasing pH from 2.0 to 10.0, a pair of redox peaks was observed in each of the CVs, and both the anodic and the cathodic peaks potential shifted negatively (Fig. 3). The anodic peak potential (E_{pa}) linearly depended on pH value varying from 2.0 to 10.0. The slope was found to be −56.4 mV/pH unit over a pH range from 2.0 to 10.0 as expected for a two-electron, two-proton electrochemical reaction. (Fig. 3, inset A). As it is shown in (Fig. 3, inset B), there was a little increase of the response in the current at lower than (pH 7.0). However, a decrease in the current above 7.0 was observed, so the higher current response may occur at this pH value. Thus, the pH of 7.0 is selected as an optimum value.

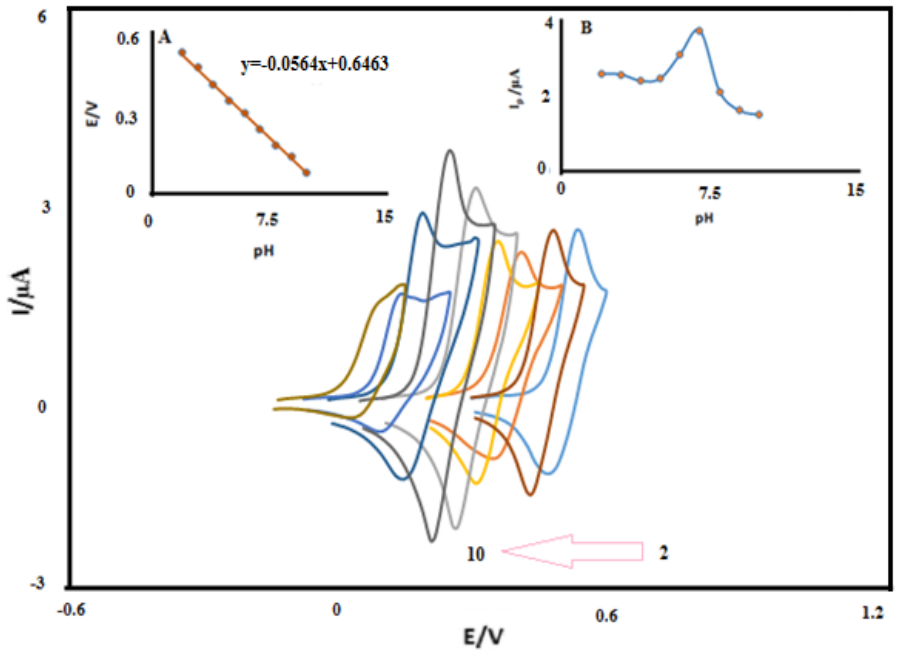

Fig. 3. CVs of DMC/NF/CP in different pH values of 2-10 the insets A and B, show effects of pH on the anodic peak potential and anodic peak current in phosphate buffer solution Scan rate 50 mV s^{-1}

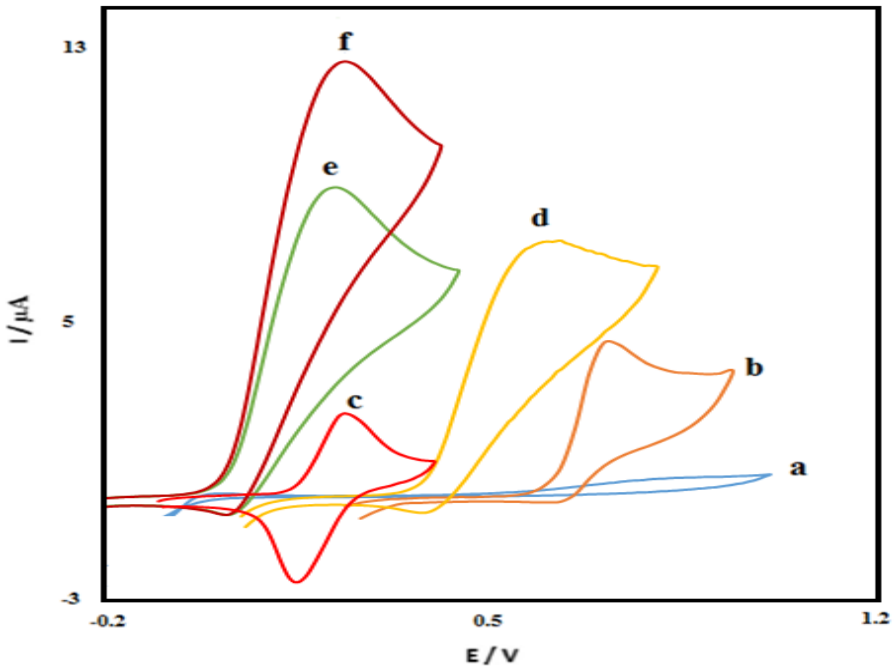

Fig. 4. CVs of (a) unmodified CPE in 0.1 M phosphate-buffered solution (pH 7.0) at scan rate of 15 mVs^{-1};(b) as (a)+0.3 mM Trp.; (c) as (a) at the surface of DMC/NF/CP; (d) as (b) at the surface of NF/CP; (e) as (b) at the surface of DMC/CP, (f) as (b) at the surface of DMC/NF/CP

3.4. Electrocatalytic oxidation of tryptophan at the surface of DMC/NF/CP

Fig. 4 shows the cyclic voltammograms of unmodified CPE in 0.1 M PBS (pH 7.0) (curve a), unmodified CPE in the presence of 300 μM Trp. (curve b), DMC/NF/CP (curve c) in PBS, the oxidation of 300 μM Trp. at NF/CP (curve d), DMC/CP (curve e) and DMC/NF/CP (curve f). At a bare electrode, the direct oxidation of tryptophan is not significant, and a small anodic current and positive peak potential due to the oxidation of Trp. are observed. However, if the electrode is modified with DMC/NF/CP, and then placed in the electrochemical cell containing Trp., a large anodic peak and a negative shift in potential are observed with cathodic peak current decreasing accordingly. Therefore, it can be indicated an electrocatalytic process has occurred. As it is seen, while the anodic peak potential for Trp. oxidation at the NF/CP and unmodified CPE is 605, and 720 mV, respectively, the corresponding potential at DMC/NF/CP is ∼230 mV. These results indicate that the peak potential for Trp. oxidation at the electrode shifts by ∼373 and 490 mV, toward negative values compared to NF/CP and unmodified CPE, respectively. However, DMC/NF/CP shows much higher anodic peak current for the oxidation of Trp. compared to unmodified CPE, indicating that the combination of NFs and the mediator (DMC) has significantly improved the performance of the electrode toward Trp. oxidation.

3.5. Effect of scan rate on the peak current

The effect of scan rate on the electrocatalytic oxidation of Trp. at the modified electrode was investigated by CV (Fig. 5). As it can be observed in Fig. 5, the oxidation peak potential shifted to more positive potentials with increasing scan rate, confirming the kinetic limitation in the electrochemical reaction. As it is shown in (Fig. 5, inset A) the anodic peak current (I_{pa}) of Trp. increased with increasing scan rate on the modified electrode in pH 7.0 phosphate buffer and exhibited a linear relation to the square root of the scan rate, $v^{1/2}$, in the range of 5–40 mV s^{-1}. The result indicates that the electron transfer reaction is controlled by the diffusion of Trp. A plot of the scan rate-normalized current ($I_p/v^{1/2}$) versus scan rate (Fig. 5, inset B) exhibits the characteristic shape typical of an $E\acute{C}_{cat}$ process [38]. If deprotonation of Trp. is a sufficiently fast step, the number of electrons involved in the rate-determining step can be estimated from the slope of the Tafel plot. The inset C of Fig. 5 shows a Tafel plot that was drawn from points of the Tafel region of the CV. The Tafel slope of 0.114 $Vdecade^{-1}$ obtained in this case agrees well with the involvement of one electron in the rate-determining step of the electrode process, assuming a charge transfer coefficient of α=0.5.

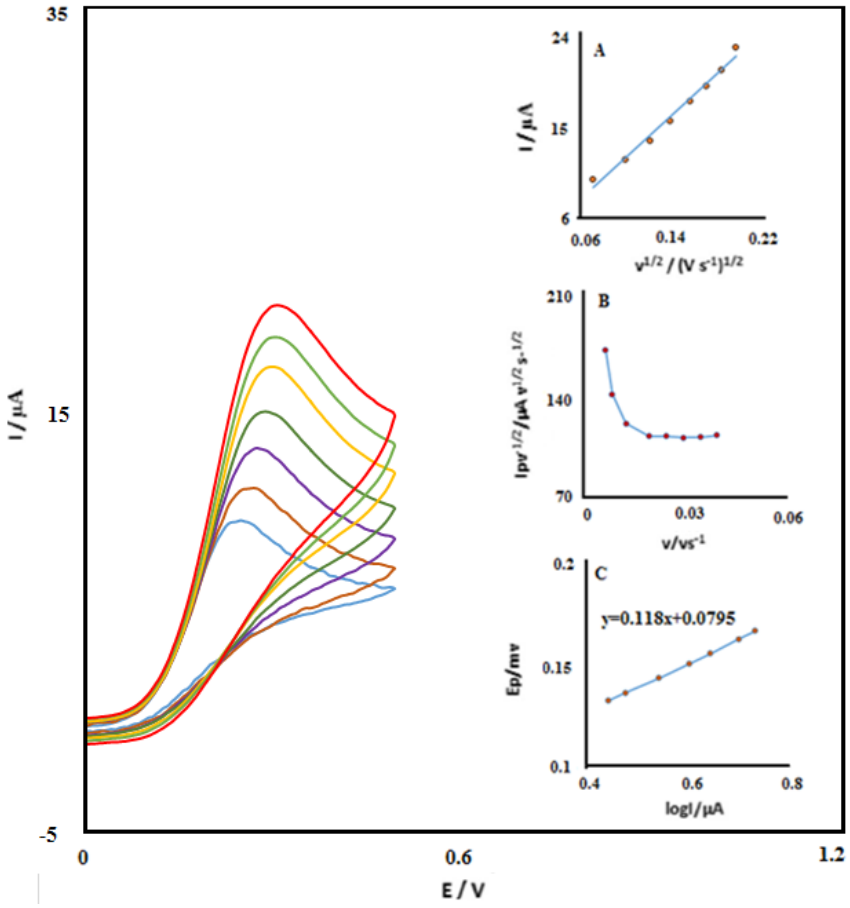

Fig. 5. CVs DMC//NF/CP in 0.1 M phosphate buffered solution (pH 7.0) containing 0.3 mM Trp. at various scan rates, from inner to outer scan rates of 5, 10, 15, 20, 25, 30, and 40 mV s^{-1}, respectively. Insets: variation of (A) anodic peak current versus $\upsilon^{1/2}$; (B) normalized current ($I_p/\upsilon^{1/2}$) versus υ; (C) Tafel plot derived from the rising part of voltammogram recorded at a scan rate of 10 mV s^{-1}

The chronoamperometric behavior of Trp. was examined at modified CPE in the presence of various concentration of Trp.. solution by setting the working electrode potential at 300 mV at the first potential steps (Fig. 6). For an electroactive compound (Trp. in this case) with an apparent diffusion coefficient, D_{app}, the current observed for the electrochemical reaction at the mass transport limited condition is described by Cottrell equation [38]:

$$I=nFAD^{1/2}C\pi^{-1/2}t^{-1/2} \quad (2)$$

The Cottrell plots of I *vs.* $t^{-½}$ were used, with the best fits for different concentrations of Trp. (Fig. 6, Inset A). The slopes of the resulting straight lines were then plotted *vs.* Trp. concentrations (Fig. 6, Inset B). The value of the D was found to be 0.45×10^{-6} cm^2 s^{-1} from the resulting slope and Cottrell equation. We designate the obtained value as an apparent diffusion coefficient, since we believe that in the experimental conditions the diffusion of

Trp. from solution bulk to electrode surface can be affected to some extent by the rate of electron transfer between substrate and modifier. However, the calculated value of the diffusion coefficient is in good agreement with those previously reported [39].

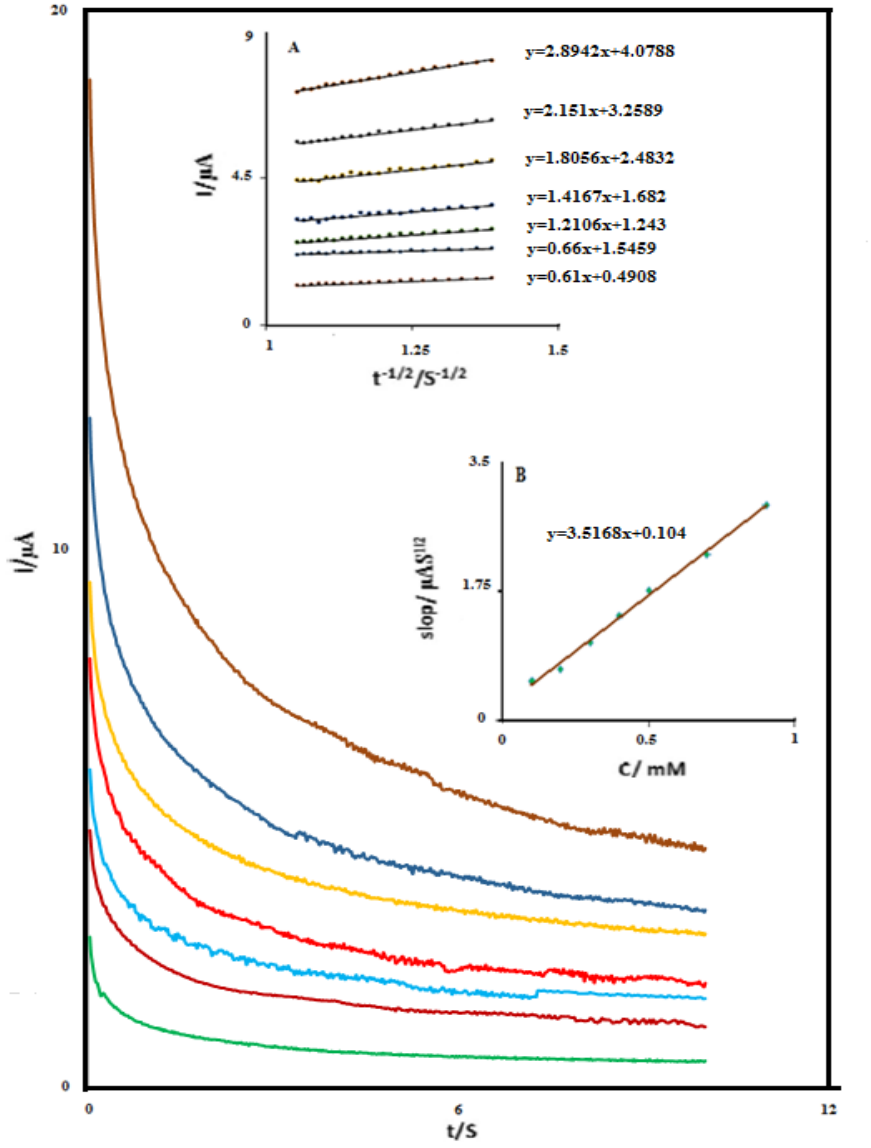

Fig. 6. (A) Chronoamperometric response of DMC/NF/CP in 0.1M phosphate buffer solution (pH 7.0) at potential step of 300 mV for different concentration of Trp.. The numbers of 1–7 correspond to 0.1, 0.2, 0.3, 0.4, 0.5, 0.6 and 0.7 mM Trp.. Insets: (A) Plots of I *vs.* $t^{-1/2}$ obtained from the chronoamperograms 1–7 and (B) plot of the slopes of the straight lines against the Trp. Concentration

The rate constant for the chemical reaction between Trp. at the surface of DMC/NF/CP, k_h, can be evaluated by chronoamperometry according to the method of Gallus [38]:

$$I_C/I_L = \gamma^{1/2}[\pi^{1/2}\mathrm{erf}(\gamma^{1/2}) + \exp(-\gamma)/\gamma^{1/2}] \quad (3)$$

Where I_C is the catalytic current of Trp. at the DMC/NF/CP, I_L the limited current in the absence of Trp. and $\gamma=kC_bt$ (C_b is the bulk concentration of Trp.) is the argument of the error function. In the cases where γ exceeds 2 the error function is almost equal to 1 and therefore the above equation can be reduced to:

$$I_C/I_L=\pi^{1/2}\gamma^{1/2}=\pi^{1/2}(kC_bt)^{1/2} \quad (4)$$

The calculated k_h value for Trp. was 5.94×10^{2} $M^{-1}s^{-1}$ using the slope of I_C/I_L versus $t^{1/2}$ plot.

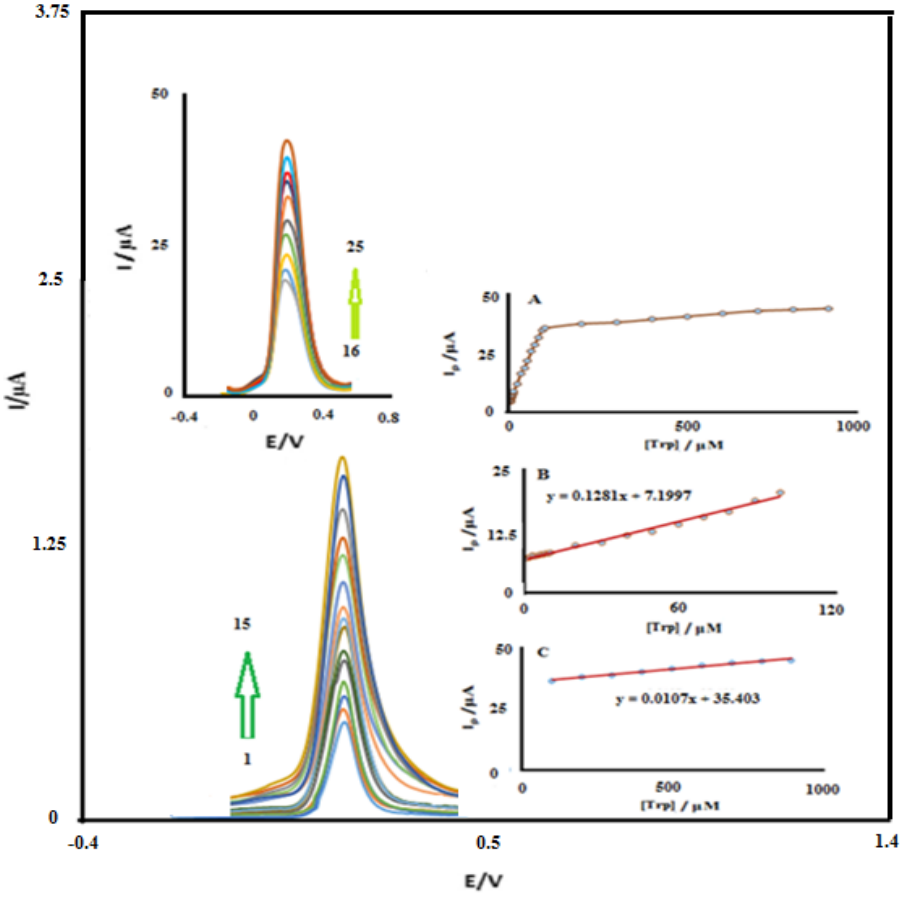

Fig. 7. Differential pulse voltammograms of DMC/NF/CP in 0.1 M phosphate buffer solution (pH 7.0) containing different concentrations of Trp. The numbers of 1–25 correspond to 1.0, 2.0, 3.0, 4.0, 5.0, 6.0, 7.0, 8.0, 9.0, 10.0, 20.0, 30.0, 40.0, 50.0, 60.0, 70.0, 80.0, 90.0, 100.0, 200.0, 300.0, 400.0, 500.0, 600.0, 700.00 and 900.0 μM Trp. Insets show the plots of the electrocatalytic peak current as a function of Trp. concentration in the range of (A) 1.0-900.0, (B) 1.0–100.0 μM and (B) 100.0–900.0 μM

3.6. Determination of Trp. by differential pulse voltammetry (DPV)

DPV was used for the determination of Trp. at the DMC/NF/CP because of its higher current sensitivity and better resolution than cyclic voltammetry. The results are shown in

Fig. 7. From Fig. 7, inset A, the peak current of Trp. is positively proportional to the Trp. concentration, in the range of 1.0–900.0 μM indicating that the calibration plots is constituted from two linear segments with different slopes, corresponding to two different ranges of 1.0–100.0 μM (Fig. 7, inset B) and 100.0 to 900.0 μM (Fig. 7, inset C) of Trp. concentration. In the second linear range (higher Trp. concentrations), the decrease of sensitivity (slope) can likely happens dues to a kinetic limitation. The peak current values showed a strong linear correlation with Trp. concentration, I_p (μA)=0.1281x+7.199, displaying an r^2 value of 0.991 with a limit of detection (based on 3σ) for Trp. of 1.03×10^{-7} M.

3.7. Response of Trp. in the presence of PA and FA

The simultaneous determination of Trp., PA and FA using a DMC/NF/CP has not been reported, so the main purpose of this study was to detect Trp., PA and FA simultaneously using carbon paste electrode modified with DMC and Titania nanofibers.

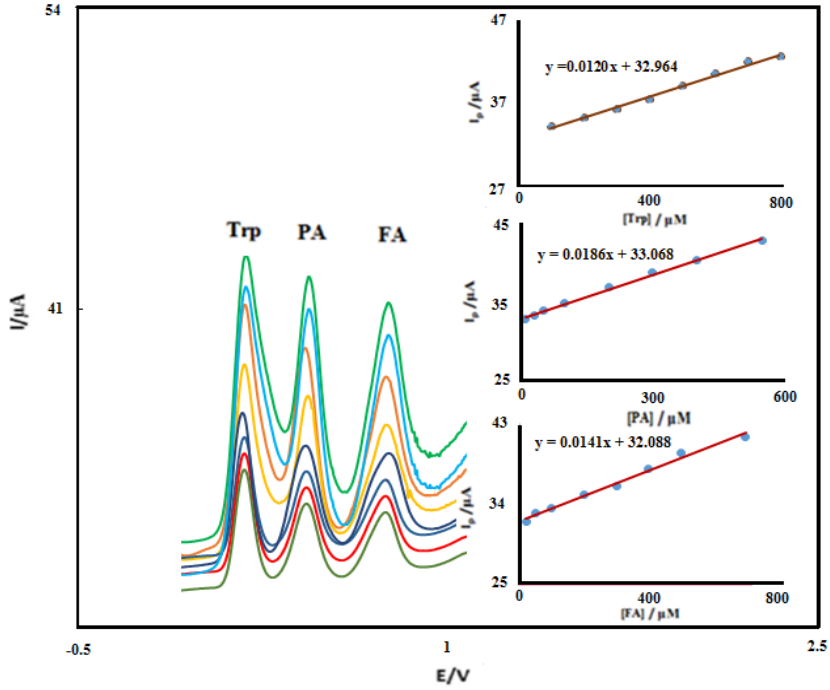

Fig. 8. DPVs of DMC/NF/CP in 0.1 M phosphate buffer solution (pH 7.0) containing different concentrations of Trp.+PA+FA in μM (from inner to outer): mixed solutions of 20.0+10.0+20.0, 70.0+30.0+50.0, 120.0+50.0+100.0, 250.0+100.0+200.0, 350.0+200.0+300.0, 450.0+300.0+400.0, 550.0+400.0+500.0 and 750.0+550.0+700.0, respectively. Insets: (A–C) plots of the peak currents as a function of Trp., PA and FA concentration, respectively

This was achieved by simultaneously changing the concentrations of Trp., PA and FA, and recording DPVs, as shown in Fig. 8. DPVs showed well-defined anodic peaks at

potentials of 195, 449 and 776 mV, corresponding to the oxidation peak potential of Trp., PA and FA, respectively. The sensitivities of the modified electrode towards the oxidation of Trp. (Range: 100.0-800.0 μM), PA and FA were found to be 0.012 $\mu A \mu M^{-1}$ (Inset A of Fig. 8), 0.0186 $\mu A \mu M^{-1}$ (Inset B of Fig. 8) and 0.0141 $\mu A \mu M^{-1}$ (Inset C of Fig. 8), respectively. No changes in the peak currents and potentials of Trp. oxidation when Trp., PA and FA can be found and their higher concentrations in same buffer solutions. No interference can be observed for the determination of Trp. by the coexisting other three species (Trp., PA and FA). All the results identifies that it is possible to selective detection of Trp. from its interferences in samples at the DMC/NF/CP. Therefore, simultaneous determination of Trp., PA and FA at the DMC/NF/CP has been done easily and perfectly. The comparison of the DMC/NF/CP, with other modified electrodes, especially those electrodes based on carbon materials, for Trp. determination was listed in Table S1. These results indicated that the DMC/NF/CP is an appropriate platform for the determination of Trp.. More importantly, one dimension (1D) nanostructures have the advantages of low production cost and facile preparation procedure over other carbon materials.

3.8. Tolerance of foreign substances

The possible interference for Trp. voltammetric determination at the DMC/NF/CP was investigated. The tolerance limit was taken as the maximum concentration of the foreign substances which caused a relative error of approximately ±5% in the determination. Ascorbic acid, uric acid and some available amino acids (5 mM), including L-cysteine, L-glutamic acid, L-tyrosine, L-serine, L-arginine and L-glycine, had no influence on the current response for 1.0 mM Trp.

3.9. Determination of Trp. in pharmaceutical samples

The modified carbon paste electrode was utilized to determine Trp., PA and FA in real samples. The results are presented in Table S2. In order to evaluate the reliability of the proposed method for the determination of Trp., a recovery test was carried out by adding known amounts of Trp., PA and FA to the human blood serum samples while sample were found to be free from Trp., PA and FA. The recoveries obtained ranged from 91.0% to 106 %, indicating that the modified electrode is reliable for the quantification of Trp.

4. CONCLUSIONS

DMC/NF/CP was prepared and used for the investigation of the electrochemical properties of Trp. The peak current increased obviously and the peak potential shifted negatively compared with unmodified CPE, indicating that modified electrode has excellent electrocatalytic activity and voltammetric response towards Trp. determination in

physiological condition. The electrochemical oxidation peak current of Trp. was linearly depended on its concentrations and the calibration curve was obtained in the ranges 1.0-900.0 μM with DPV method, and detection limit (3σ) was determined as 1.03×10^{-7} M. The excellent analytical performance can be corresponded to good biocompatibility and high conductivity of nanofibers, which perfectly regulate the surface chemistry. These excellent properties would promote the potential applications of nanofibers-based materials in electrochemical sensors. Finally, the modified electrode was successfully applied to determination of tryptophan in human blood serum samples.

Acknowledgments

The authors wish to thank the Yazd University Research Council, IUT Research Council and Excellence in Sensors for financial support of this research.

REFERENCES

[1] F. Valentini, and G. Palleschi, Anal. Lett. 41 (2008) 479.
[2] G. M. Whitesides, Small 1 (2005) 172.
[3] M. Mazloum-Ardakani, M. Yavari, and A. R. Khoshroo, J. NanoStructures 3 (2013) 17.
[4] M. Mazloum-Ardakani, N. Rajabzadeh, A. Dehghani-Firouzabadi, A. Benvidi, B. B. F. Mirjalili, and L. Zamani, J. Electroanal. Chem. 760 (2016) 151.
[5] M. Mazloum-Ardakani, F. Sabaghian, A. Khoshroo, and H. Naeimi, Chinese J. Catal. 35 (2014) 56.
[6] O. J. D'Souza, R. J. Mascarenhas, T. Thomas, B. M. Basavaraja, A. K. Saxena, K. Mukhopadhyay, and D. Roy, J. Electroanal. Chem. 739 (2015) 49.
[7] M. Mazloum-Ardakani, and M. A. Sheikh-Mohseni, Anal. Bioanal. Electrochem. 6 (2014) 106.
[8] Z. M. Huang, Y. Z. Zhang, M. Kotaki, and S. Ramakrishna, Compos. Sci. Technol. 63 (2003) 2223.
[9] J. D. Schiffman, and C. L. Schauer, Polym. Rev. 48 (2008) 317.
[10] D. Li, J. T. McCann, Y. Xia, and M. Marquez, J. Am. Ceram. Soc. 89 (2006) 1861.
[11] J. Huang, Y. Liu, and T. You, Anal. Methods 2 (2010) 202.
[12] H. Fong, I. Chun, and D. H. Reneker, Polymer (Guildf). 40 (1999) 4585.
[13] C. Zhang, X. Yuan, L. Wu, and Y. Han, J. Sheng, Eur. Polym. J. 41 (2005) 423.
[14] R. J. Reiter, Exp. Gerontol. 30 (1995) 199.
[15] H. Li, F. Li, C. Han, Z. Cui, G. Xie, and A. Zhang, Sens. Actuators B 145 (2010) 194.
[16] M. Tedetti, P. Joffre, and M. Goutx, Sens. Actuators B 182 (2013) 416.
[17] M. Keyvanfard, M. Tahmasbi, H. Karimi-Maleh, and K. Alizad, Chinese J. Catal. 35 (2014) 501.

[18] C. Wang, X. Zou, X. Zhao, Q. Wang, J. Tan, and R. Yuan, J. Electroanal. Chem. 741 (2015) 36.
[19] S. Kim, S. Sun, Y. Li, and X. He, Anal. Methods 7 (2015) 6352.
[20] Z. Taleat, A. Khoshroo, and M. Mazloum-Ardakani, Microchim. Acta 161 (2014) 865.
[21] A. A. Ensafi, H. Karimi-Maleh, and S. Mallakpour, Electroanalysis 23 (2011) 1478.
[22] M. Mazloum-Ardakani, M. Sheikh-Mohseni, and B. F. Mirjalili, Ionics (Kiel). 20 (2014) 431.
[23] M. Opallo, and A. Lesniewski, J. Electroanal. Chem. 656 (2011) 2.
[24] M. Mazloum-Ardakani, and A. Khoshroo, Electrochim. Acta 130 (2014) 634.
[25] M. Mazloum-Ardakani, L. Hosseinzadeh, A. Khoshroo, H. Naeimi, and M. Moradian, Electroanalysis 26 (2014) 275.
[26] H. I. Mosberg, R. Hurst, V. J. Hruby, K. Gee, H. I. Yamamura, J. J. Galligan, and T. F. Burks, Proc. Natl. Acad. Sci. 80 (1983) 5871.
[27] R. Gotti, R. Pomponio, V. Andrisano, and V. Cavrini, J. Chromatogr. A 844 (1999) 361.
[28] A. A. Elbashir, S. F. Awad, J. Pharmacovigil. 1 (2013) 2.
[29] L. Song, Z. Guo, and Y. Chen, Electrophoresis 33 (2012) 2056.
[30] L. Ma, M. Fan, X. Xu, W. Kang, and H. Shi, J. Braz. Chem. Soc. 22 (2011) 1463.
[31] M. Mazloum-Ardakani, M. A. Sheikh-Mohseni, and B. Mirjalili, Electroanalysis 25 (2013) 2021.
[32] A.A. Ensafi, E. Khoddami, B. Rezaei, and H. Karimi-Maleh, Colloids Surfaces B 81 (2010) 42.
[33] G. G. Klee, Clin. Chem. 46 (2000) 1277.
[34] M. Mazloum-Ardakani, A. Khoshroo, D. Nematollahi, and B. F. Mirjalili, J. Electrochem. Soc. 159 (2012) H912.
[35] R. Chandrasekar, L. Zhang, J. Y. Howe, N. E. Hedin, Y. Zhang, and H. Fong, J. Mater. Sci. 44 (2009) 1198.
[36] M. Mazloum-Ardakani, and A. Khoshroo, J. NanoStructures 3 (2013) 269.
[37] E. Laviron, J. Electroanal. Chem. Interfacial Electrochem. 101 (1979) 19.
[38] A. J. Bard, L. R. Faulkner, Electrochemical Methods: Fundamentals and Applications, 2nd ed., Wiley, (2000).
[39] M. Mazloum-Ardakani, R. Arazi, H. Beitollahi, and H. Naeimi, Anal. Methods 2 (2010) 1078.